ESC Cardiovascular Research (2026) **122**, 397–411
https://doi.org/10.1093/cvr/cvag017

Maresin 1 ameliorates myocardial ischaemia–reperfusion injury by promoting tissue resident macrophage efferocytosis

Xuan Sun [1], Yuting Feng[2], Yawei Zhao[1], Yue Cai[1], Zhenzhu Cao[3], Yu Zhang[3], Zhonghai Wei[1], Anning Du [1], and Biao Xu [1]*

[1]Department of Cardiology, Nanjing Drum Tower Hospital, Medical School of Nanjing University, Nanjing Key Laboratory for Cardiovascular Information and Health Engineering Medicine, No. 321 Zhongshan Road, Nanjing 210008, China; [2]Tongren Hospital, Shanghai Jiao Tong University School of Medicine, No. 1111 XianXia Road, Shanghai 200336, China; and [3]Department of Cardiology, Nanjing Drum Tower Hospital, Nanjing Drum Tower Hospital Clinical College of Nanjing University of Chinese Medicine, 358 Zhongshan Road, Nanjing 210008, China

Received 20 June 2025; revised 30 October 2025; accepted 26 November 2025; online publish-ahead-of-print 20 January 2026

Time of primary review: 23 days

Aims Myocardial ischaemia–reperfusion (I/R) injury triggers a robust inflammatory storm cascade that critically compromises reperfusion efficacy following acute myocardial infarction. Enhanced efferocytosis by cardiac resident macrophages (RMs) has therapeutic potential for inflammation resolution. The unsaturated long-chain fatty acid Maresin1 (MaR1) exhibits potent anti-inflammatory properties that is devoid of immunosuppressive effects. However, its therapeutic potential in myocardial I/R injury and regulatory mechanisms in cardiac RMs remains unexplored.

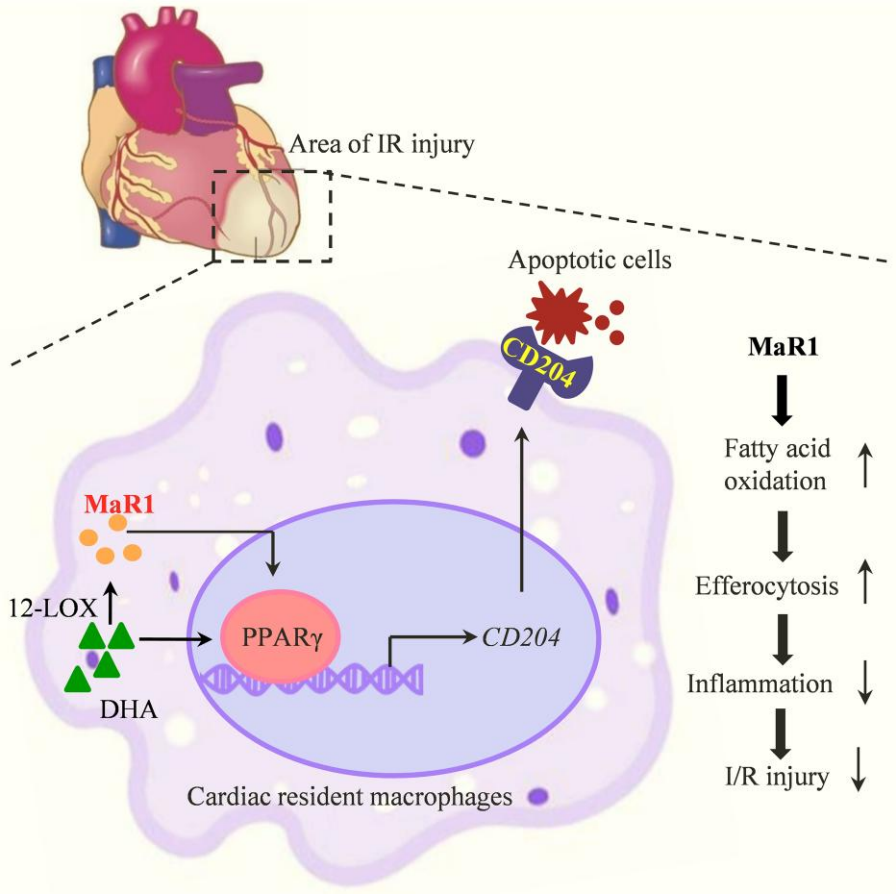
Methods and results A clinical case–control study was conducted and revealed a negative association between circulating MaR1 levels and inflammatory markers and the severity of I/R injury in patients with ST-elevation myocardial infarction. Mice treated with MaR1 after myocardial I/R injury showed improvements in cardiac function and efferocytosis by cardiac RMs. Genetic ablation of cardiac RMs abolished MaR1-mediated cardioprotection. To explore the mechanism underlying this protection, we performed transcriptomic, metabolomics, and lipidomic analyses and identified fatty acid β-oxidation potentiation as a key metabolic signature in MaR1-treated RMs. Moreover, MaR1 directly bound peroxisome proliferator-activated receptor γ (PPARγ), inducing the transcriptional activation of its downstream efferocytosis-related target CD204. Specific knockout of PPARγ in RMs significantly attenuated MaR1-enhanced efferocytosis. Notably, oral supplementation with the MaR1 precursor docosahexaenoic acid (DHA) recapitulated these cardioprotective effects.

Conclusion Our findings prove that MaR1 plays a protective role in myocardial I/R injury by facilitating efferocytosis by RMs and the resolution of inflammation. These results offer novel therapeutic perspectives for the management of myocardial I/R injury.

Downloaded from academic.oup.com/cardiovascres/article/122/3/397/8430176 by Ewha Womans University Library - (INACTIVE) user on 28 August 2026

* Corresponding author. Tel/fax:+86-025-68182812, Email: xubiao62@nju.edu.cn
© The Author(s) 2026. Published by Oxford University Press on behalf of the European Society of Cardiology. All rights reserved. For commercial re-use, please contact reprints@oup.com for reprints and translation rights for reprints. All other permissions can be obtained through our RightsLink service via the Permissions link on the article page on our site—for further information please contact journals.permissions@oup.com.

Graphical Abstract



The present study shows that administration of MaR1 promotes the efferocytosis in cardiac RMs by increasing PPARγ-CD204 activation and promoting fatty acid β-oxidation, thus resolving inflammation following I/R injury. DHA can exert a myocardial protective effect by being metabolized into MaR1 via the action of the alox12 enzyme. Therefore, our study reveals the critical role of MaR1 in promoting cardiac repair through the regulation of cardiac RMs, and identifies a promising therapeutic target for managing I/R injury.

Keywords Maresin 1 • Resident macrophage • Efferocytosis • Myocardial I/R injury • Inflammation

1. Introduction

Acute myocardial infarction (AMI) represents one of the most severe cardiovascular diseases (CVDs) in modern society and is associated with the highest rates of mortality and disability. While timely reperfusion is essential for restoring ischaemic heart tissue, it paradoxically induces permanent myocardial damage, referred to as myocardial ischaemia–reperfusion (I/R) injury. Accumulating evidence indicates that the inflammatory response plays a pivotal role in the pathophysiology of I/R injury.[1] Active regression of the inflammatory response can successfully prevent tissue damage and adverse myocardial remodelling, which is crucial for therapeutic treatment.[1] Nevertheless, existing anti-inflammatory therapies targeting I/R injury have not yielded satisfactory results, highlighting the need for novel strategies in the treatment of ischaemic heart disease.

Macrophages play a crucial role in the inflammatory response following cardiovascular injury.[2] It is generally believed that the infiltration of inflammatory macrophages after myocardial injury exerts detrimental effects.[3] However, a growing body of evidence suggests that cardiac macrophages represent a highly heterogeneous and functionally diverse population of cells.[4] Cardiac resident macrophages (RMs) are embryonically established and maintained as a self-renewing population.[5] During the steady state, cardiac RMs contribute significantly to maintaining heart homeostasis.[6] Notably, cardiac RMs exhibit superior phagocytic capacity for cardiomyocyte debris than do circulating macrophages.[7] Efficient clearance and degradation of apoptotic cells by macrophages (efferocytosis) is essential for cardiac homeostasis and repair.[8] As a result, efferocytosis by cardiac RMs contributes significantly to maintaining the cardiac microenvironment. With advancements in metabolomics, researchers have recognized that mitochondrial energy metabolism determines the phenotype and functionality of macrophages.[9] Moreover, efferocytosis plays an important role in the metabolic reprogramming of mitochondria in macrophages.[10,11] In turn, mitochondrial metabolic pathways and metabolites influence the sustained efferocytosis and reparative functions of macrophages by supplying essential energy and substrates.[12] In this context, identifying novel drugs to enhance efferocytosis, particularly in cardiac RMs, could provide promising anti-inflammatory therapeutic strategies for myocardial I/R injury.

The resolution of inflammation is known to be mediated mainly by metabolites termed specialized proresolving lipid mediators (SPMs),

Downloaded from academic.oup.com/cardiovascres/article/122/3/397/8430176 by Ewha Womans University Library - (INACTIVE) user on 28 August 2026

which are synthesized from ω-3 polyunsaturated fatty acids (PUFAs), including eicosapentaenoic acid (EPA) and docosahexaenoic acid (DHA). Previous study reported that DHA intake dominated splenocardiac resolving phase with the biosynthesis of SPMs in heart failure mice.[13] Maresin 1 (MaR1), a member of the DHA-derived mediator family, is one of the earliest lipid mediators to respond to inflammatory signals.[14] Furthermore, the stereoselectivity of MaR1 confers its potent protective effects on local inflammation resolution.[15] Han et al. reported that MaR1 prevents steatohepatitis by the regulation of liver Kupffer macrophages.[16] However, whether MaR1 can regulate the activity of cardiac RMs and its potential influence on the progression of myocardial I/R remain unknown.

In this study, we found that plasma levels of MaR1 were associated with inflammatory markers and the severity of I/R injury in patients with ST-elevation myocardial infarction (STEMI). Moreover, the administration of MaR1 promoted efferocytosis in cardiac RMs by enhancing the fatty acid β-oxidation (FAO) pathway, thus improving cardiac repair following I/R injury. Peroxisome proliferator-activated receptor gamma (PPARγ), a lipid nuclear transcription factor, was identified as a critical mediator of MaR1 in cardiac RMs. Additionally, MaR1 enhances the transcription of the efferocytic receptor CD204 by facilitating the nuclear translocation of PPARγ, thereby retarding the inflammatory response. Finally, we confirmed the protective effects of DHA in myocardial I/R injury.

2. Methods

The detailed methods are provided in the Supplementary material online. All data supporting this study are available from the corresponding author upon reasonable request.

2.1 Human studies

Human blood samples were obtained from 55 STEMI patients who were subjected to the primary percutaneous coronary intervention (PPCI) and admitted to the Department of Cardiology at Nanjing Drum Tower Hospital. Blood samples from 20 age-matched healthy people without cardiovascular diseases were offered by the Physical Examination Center of Nanjing Drum Tower Hospital and were used as controls. The study was approved by the Institutional Ethics Committee of Nanjing Drum Tower Hospital (Approval No. 2021-531-02) according to the Helsinki declaration, and written informed consent was obtained from all participants. The demographic and clinical data of the controls and patients with STEMI are shown in Supplementary material online, *Table S1*. The blood sample of subjects was collected immediately at the time of admission, before PCI reperfusion. Specimens of EDTA anticoagulated blood were gathered and stand at room temperature for 30 min. Platelet-depleted plasma was harvested by centrifugation at 300 g for 20 min at 4°C. Maresin 1 (MaR1) levels were measured by commercial assay kits according to the manufacturer's instructions (501150, Cayman, USA).

2.2 Animals

Wild type (WT) C57BL6/J mice (male, 8 weeks old; Gem Pharmatech Co. Ltd., Jiangsu, China) were used in this study. $Cx3cr1^{creERT2}$ mice (B6.129P2(Cg)-$Cx3cr1^{tm2.1(cre/ERT2)Litt/WganJ}$, JAX: 020940); $Rosa26^{Td}$ mice (B6.CgGt(ROSA)26 $Sor^{tm14(CAG-tdTomato)Hze/J}$, JAX: 007914); $Rosa26^{iDTR}$ mice (C57BL/6-Gt(ROSA)26$Sor^{tm1(HBEGF)Awai/J}$, JAX: 007900); and $PPAR\gamma^{fl/fl}$ mice (B6.129-$Pparg^{tm2Rev/J}$, JAX:004584) were purchased from Jackson Laboratory. Another $Cx3cr1^{Td\text{-}creERT2}$ mice [C57BL/6Smoc-$Cx3cr1^{em1(2A–tdTomato-IRES-CreERT2-WPRE- pA)}$, Cat: NM-KI-242749] were purchased from Shanghai Model Organisms Center, Inc. We utilized $Cx3cr1^{creERT2}$ mice crossed with $Rosa26^{Td}$ mice to generate RM^{Td} mice, which allows tracking of RMs by tamoxifen (TM) administration, as previously described.[17] The RM^{Td} mice without TM treatment were used for the littermate controls. Then RM^{Td} mice were crossed with $Rosa26^{iDTR}$ mice to generate $Rosa26^{Td\text{-}DTR}$ mice. According to the previous study,[18] we crossed $Cx3cr1^{creERT2}$ mice with $Rosa26^{Td\text{-}DTR}$ mice to generate an $RM^{Td\text{-}DTR}$ mouse strain, which allows tracking and depletion of RMs upon diphtheria toxin (DT) administration. The $RM^{Td\text{-}DTR}$ mice without DT treatment were used for the littermate controls. $PPAR\gamma^{fl/fl}$ mice were crossed with $Cx3cr1^{Td\text{-}creERT2}$ mice to generate $PPAR\gamma^{cko}$ mice with PPARγ deletion in tdTomato-expressing RMs following TM administration. All the mice were fed a standard laboratory diet with free access to food and water and were maintained at a constant temperature (25°C) and humidity (65–70%) controlled room with a 12-h light–dark cycle. A myocardial I/R injury model was established in mice. Briefly, the mice were anaesthetized by the intraperitoneal administration of ketamine (100 mg/kg) and xylazine (10 mg/kg). The mice then underwent a ligation of the left anterior descending coronary artery (LAD) with a 7-0 silk ligature over a 1-mm polyethylene tube (PE-10) for 45 min before reperfusion. Upon successful reperfusion, 5 μg/kg (body weight) Maresin 1 (MaR1; HY-116429, MCE) per mouse was administered into the peri-infarct myocardial region for a total of 10 μL.[16] In the sham-operated group, the mice only underwent thoracotomy without ligation. In a set of experiments, DHA (HY-B2167, MCE) was dissolved in 5% gum arabic solution and administered orally once a day for 1 week (50 mg/kg/day) before I/R injury modelling.[19] To induce gene recombination in $Cx3cr1^{creERT2}$ mice, 5 mg of tamoxifen per mouse was administered (T5648, Sigma) i.p. for 5 consecutive days at the age of 3 weeks (25 mg total), as previously described. Four weeks after tamoxifen injection, 8-week-old mice were used for experimental modelling. For RM depletion, diphtheria toxin (DT; D0564, Sigma) was intraperitoneally administered to the mice (500 ng daily, 3 consecutive days) before I/R induction. After the study, all the mice were euthanized with an overdose of pentobarbital sodium (200 mg/kg, i.v.). All procedures were approved by the Institutional Ethics Committee of Nanjing Drum Tower Hospital (Approval No. 2020AE01066) and performed following the guidelines of directive 2010/63/EU of the European Parliament on the protection of animals used for scientific purposes.

2.3 Statistical analysis

Statistical analyses were performed using GraphPad Prism (version 8), and the results are presented as the mean ± standard deviations. The normality of the data was evaluated by the Shapiro–Wilk test. The homoscedasticity of the data was examined with the Bartlett and Brown–Forsythe test. For normally distributed data, statistical comparisons between two groups were conducted by the unpaired Student *t*-test, whereas comparisons across multiple groups were executed using either a one-way or two-way ANOVA followed by the Bonferroni correction. For non-normally distributed data, comparisons were performed by the Mann–Whitney *U* test or the Kruskal–Wallis test followed by Dunn's multiple comparison test. A significance level of $P < 0.05$ was considered statistically significant.

3. Results

3.1 The MaR1 level is associated with inflammation and the severity of I/R injury in STEMI patients

To investigate the clinical role of MaR1 in myocardial I/R injury, 55 STEMI patients and 20 healthy controls (HCs) were recruited for

Downloaded from academic.oup.com/cardiovascres/article/122/3/397/8430176 by Ewha Womans University Library - (INACTIVE) user on 28 August 2026

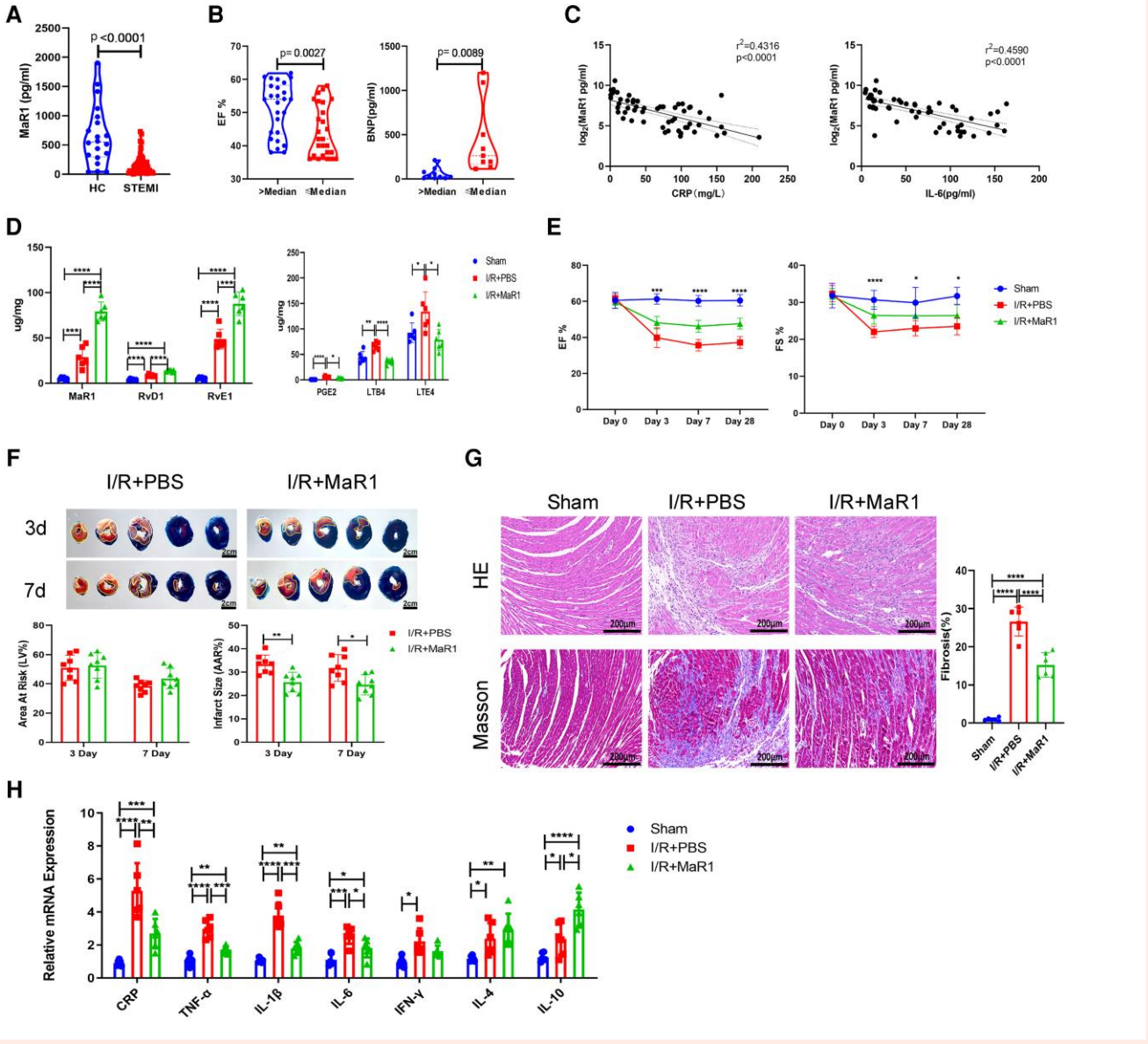


Figure 1 MaR1 supplementation alleviates myocardial I/R injury. *(A)* Quantitative levels of MaR1 in plasma of patients with STEMI ($n = 55$) or healthy control (HC) individuals ($n = 20$). *(B)* The levels of EF or BNP in plasma of patients who have MI with a MaR1 level greater than the median compared with patients with a MaR1 level less than or equal to the median ($n = 27$ for the > Median group and $n = 28$ for the ≤ Median group). *(C)* Correlation of MaR1 levels with IL-6 (X; $n = 55$) or CRP (X; $n = 55$) levels in plasma of patients with STEMI. *(D)* Quantitative analysis of proinflammatory lipid mediators (PGE2, LTB4, and LTE4) and proresolving lipid mediators (MaR1, RvD1, and RvE1) levels in murine cardiac tissues using LC-MS/MS methods at day 3 after I/R or sham operation ($n = 6$ per group). *(E)* Echocardiography measurements of cardiac function of mice at day 0, day 3, day 7, and day 28 after IR. Left ventricular EF and FS were shown at the indicated days after IR or sham operation ($n = 10$ per group). *(F)* Representative images of Evans blue and TTC double-stained sequential cardiac sections from mice. Quantitative analyses of the percentage area at risk (AAR) and percentage infarct of hearts are shown ($n = 8$ per group). Scale bar = 2 cm. *(G)* Representative images of HE and Masson trichrome staining of sequential cardiac sections from mice 3 days after I/R ($n = 6$ per group). Scale bar = 200μm. *(H)* The mRNA expression levels of genes associated with cardiac inflammation in left ventricles at day 3 after I/R ($n = 6$ per group). Data were presented as mean ± SD. (A) Student *t*-test; (B) Mann–Whitney *U* test; (C) Spearman correlation analysis; (D and H) Two-way ANOVA followed by Bonferroni test; (E) Two-way ANOVA followed by Tukey's multiple test (I/R + PBS vs. I/R + MaR1); (F–G) One-way ANOVA with Bonferroni test. $^{*}P < 0.05$, $^{**}P < 0.01$, $^{***}P < 0.005$, $^{****}P < 0.001$.

the trial. The baseline characteristics of the participants are summarized in Supplementary material online, *Table S1*. The plasma levels of MaR1 were lower in the STEMI group than in the HC group (*Figure 1A*). Patients with MaR1 levels greater than the median were subsequently defined as the '>Median' group, and those with MaR1 levels less than or equal to the median were defined as the '≤Median' group. Ejection fraction (EF) levels in the ≤Median group were significantly lower than those in the >Median group, whereas

Downloaded from academic.oup.com/cardiovascres/article/122/3/397/8430176 by Ewha Womans University Library - (INACTIVE) user on 28 August 2026

the plasma levels of BNP (B-type natriuretic peptide) in the ≤Median group were significantly greater than those in the >Median group (*Figure 1B*). Additionally, the levels of MaR1 were negatively correlated with the cardiac troponin T (cTNT) and creatine kinase M-type (CK-MB) levels in STEMI patients (see Supplementary material online, *Figure S1A*). To further explore the involvement of MaR1 in the inflammatory response following AMI, we evaluated the relationships between plasma MaR1 levels and the levels of inflammation makers, including interleukin 6 (IL-6) and C-reactive protein (CRP). According to the data, MaR1 levels were negatively correlated with IL-6 and CRP plasma concentrations in STEMI patients (*Figure 1C*). These data indicate that MaR1 levels are negatively associated with inflammation and the severity of I/R injury in STEMI patients.

3.2 MaR1 supplementation alleviates myocardial I/R injury

To investigate the therapeutic effect of MaR1 on cardiac damage, mice were given MaR1 immediately after reperfusion. Left ventricular tissues from mice 3 days after I/R injury were collected for targeted metabololipidomic profiling using liquid chromatography–tandem mass spectrometry (LC–MS/MS). Analysis of fatty acid metabolites revealed that the levels of MaR1 and other proresolving fatty acid metabolites (RvD1 and RvE1) were significantly greater in the MaR1-treated group than in the PBS-treated group post-I/R. Conversely, the levels of proinflammatory lipid metabolites (PGE2, LTB4, and LTE4) were markedly decreased in the MaR1-treated group (*Figure 1D* and *S1B*). Echocardiography assessments at individual time points demonstrated that MaR1 treatment alleviated I/R-induced dysfunction in the myocardium, as evidenced by increased left ventricular EF and fractional shortening (FS) (*Figure 1E*). Additionally, MaR1 treatment suppressed the protein expression of apoptosis-associated pathways in the cardiac tissues 3 days post-I/R (see Supplementary material online, *Figure S1C*). Subsequent analysis revealed no significant difference in the area at risk (AAR), but infarct sizes were notably decreased in the I/R + MaR1 group, as confirmed by Evans blue and TTC staining (*Figure 1F*). Pathological staining of myocardial tissues revealed reduced inflammatory cell infiltration and attenuated fibrosis in the I/R + MaR1 group compared with the I/R + PBS group 3 days post-operation (*Figure 1G*). Furthermore, the mRNA levels of proinflammatory cytokines, including CRP, TNF-α, IL-1β, and IL-6, were significantly decreased, whereas the mRNA levels of anti-inflammatory cytokines, such as IL-4 and IL-10, were substantially increased in the cardiac tissues of MaR1-treated mice 3 days post-I/R (*Figure 1H*). In addition, cardiac sections obtained from mice 28 days post-I/R revealed the long-term protective effects of MaR1 on ventricular remodelling, inflammatory infiltration and fibrosis (see Supplementary material online, *Figure S1D*). These findings indicate that MaR1 treatment facilitates the resolution of cardiac inflammation and protects against myocardial I/R injury.

3.3 MaR1 treatment activates efferocytosis of cardiac resident macrophages

Cardiac RMs are primarily of embryonic origin and play a major role in efferocytosis and inflammation resolution.[7] To investigate whether RMs are involved in the effects of MaR1, we constructed the Cx3cr1^{creERT2}; Rosa26^{Td} (termed RM^{TD}) mouse line to specifically trace RMs in the heart, as previously reported (*Figure 2A*).[20] Briefly, the mouse was intraperitoneally administered 5 mg tamoxifen for 5 consecutive days at 3 weeks of age. Four weeks after tamoxifen injection, the mice were used for experimental modelling.[17] The validity of the model was confirmed by assessing the proportions of Td$^+$ RMs in the cardiac tissues, blood and bone marrow of RM^{TD} mice (see Supplementary material online, *Figure S2A* and *B*). Flow cytometry analysis revealed a significantly decreased proportion of total CD11b$^+$CD64$^+$ macrophages and an increased proportion of Td$^+$ RMs in the I/R + MaR1 group compared with those in the I/R + PBS group at 3 days post-I/R injury (*Figure 2B*). MaR1 is known to increase the phagocytic activity of macrophages.[21] To determine the effective dose of MaR1 in vitro, we co-cultured PKH67-labelled apoptotic cells (ACs) with primary cardiac RMs treated with various concentrations of MaR1. After removing unengulfed ACs, we observed a higher proportion of PKH67$^+$ RMs in the MaR1-treated group than in the PBS-treated group, and 100 nM was the optimal dose of MaR1 for efferocytosis of RMs (see Supplementary material online, *Figure S2C* and *D*). Additionally, the terminal deoxynucleotidyl transferase-mediated dUTP-biotin nick-end labelling (TUNEL) staining of cardiac sections from RM^{TD} mice confirmed that MaR1 administration increased the number of Td$^+$ RMs while decreasing the number of TUNEL$^+$ ACs. Importantly, MaR1 treatment expanded the population of Td$^+$ TUNEL$^+$ cells, indicating that MaR1-mediated efferocytosis in RMs was enhanced (*Figures 2C* and *S2E*). To further investigate the impact of MaR1 on efferocytosis following I/R injury, we classified Td$^+$TUNEL$^+$ cells into four types according to the contact size: no touch, touch, enwrapped, and engulfed. The quantification of Td$^+$TUNEL$^+$ cells in each category revealed that MaR1 administration significantly increased the proportion of 'engulfed' RMs within the myocardium (*Figure 2D*). These data indicate that MaR1 promoted high-burden efferocytosis in macrophages. To test this hypothesis, a continual efferocytosis experiment was carried out as previously reported.[22] Primary RMs were incubated with PKH67-labelled ACs (green) for 45 min. After AC removal, the macrophages were allowed to rest for 2 h and then incubated with a second round of PKH26-labelled ACs (red). As expected, MaR1-treated RMs displayed a greater level of internalization of both labelled ACs than the control RMs did (see Supplementary material online, *Figure S2F*). Transmission electron microscopy (TEM) revealed a significant increase in the number of macrophage (purple area) phagocytic vesicles (yellow area) in the cardiac tissues from I/R + MaR1 group compared with those from the I/R + PBS group. In addition, MaR1 treatment reduced the number of unengulfed residual bodies (dark areas) in the phagocytic vesicles, which suggested increased macrophage efferocytosis by MaR1 (*Figure 2E*). Macrophage Mertk,[23] CD36,[24] and CD204[25] receptors are critical mediators of apoptotic cell recognition and phagocytosis during inflammation resolution. Therefore, we investigated whether MaR1 affects macrophage efferocytosis by regulating these receptors. We observed that the expression of CD204 was obviously increased by MaR1 treatment both in vivo and in vitro (*Figures 2F, G* and *S2G, H*), indicating that CD204 may serve as an effector of MaR1. We subsequently examined whether MaR1-treated RM exhibited anti-inflammatory and proresolving characteristics. Our findings demonstrated that the M1 macrophage markers (including iNOS, TNF-α, IL-1β, and IL-6) were significantly downregulated but that M2 macrophage markers (including IL-10, Arg1, IL-4, and CD206) were upregulated in the MaR1-treated group compared with those in the PBS group (see Supplementary material online, *Figure S2I*). Together, these results suggest that MaR1 increases the efferocytosis of cardiac RMs by coordinating corpse uptake, processing ingested materials and secreting anti-inflammatory mediators.

3.4 Resident macrophages are essential for MaR1-mediated cardiac protection

To identify the functional role of RMs in the effect of MaR1, we utilized the RM$^{TD\text{-}DTR}$ mouse strain to conditionally deplete cardiac RMs upon intraperitoneal administration of diphtheria toxin (DT; 500 ng daily for 3 consecutive days before I/R induction), as

Downloaded from academic.oup.com/cardiovascres/article/122/3/397/8430176 by Ewha Womans University Library - (INACTIVE) user on 28 August 2026

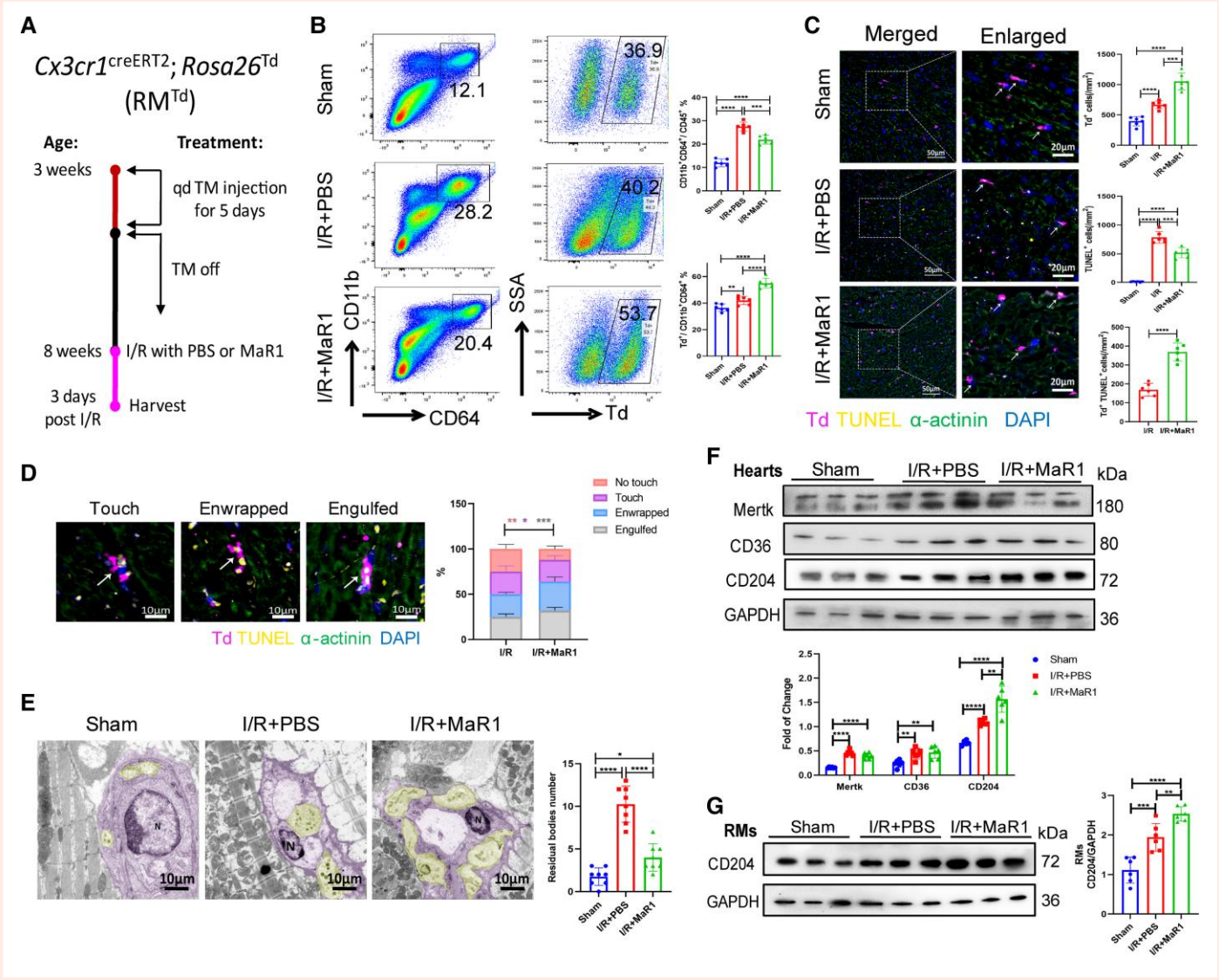


Figure 2 MaR1 treatment promotes the efferocytosis of cardiac resident macrophages. *(A)* Diagram of tamoxifen administration and myocardial I/R injury operation in Cx3cr1^{creERT2}; Rosa26^{Td} (RM^{Td}) mice. *(B)* Representative flow cytometry analysis of cardiac CD11b^{+} CD64^{+} macrophages and cardiac macrophages gated on Td^{+} cells at day 3 after I/R (n = 6 per group). The number shown in gated region is the % for the representative sample. *(C)* Representative immunofluorescence images of Td^{+} cells (RM, pink) in cardiac sections stained with apoptotic cells (TUNEL, yellow), cardiac sarcomere (α-actinin, green) and nuclei (DAPI, blue) from RM^{Td} mice at day 3 after I/R. Td^{+} cells and apoptotic cells colocalization indicated efferocytosis of cardiac resident macrophages. Quantifications of Td^{+} cells, TUNEL^{+} cells and Td^{+} TUNEL^{+} cells were shown on right (n = 6 per group). Scale bar: left = 50μm; right = 10μm. *(D)* Td^{+} cells were classified into four types according to their contact with apoptotic cells immunosignal as shown in images: no touch, touch, enwrapped and engulfed. Scale bar = 10μm. Percentages of each types cells were shown on right (n = 6 per group). *(E)* Representative TEM images of the macrophage (purple area) swallowing the debris in cardiac tissues at day 3 after I/R. Residual bodies can be identified by higher electrodensity (dark areas) in the phagocytic vesicles (yellow area). 'N' represents the cell nucleus. Scale bars =10 μm. *(F)* Immunoblot analysis of efferocytosis receptors proteins in murine cardiac tissues at day 3 after I/R (n = 6 per group). GAPDH was used as the loading control. *(G)* Immunoblot analysis of CD204 proteins in the RMs sorted from murine hearts at day 3 after I/R (n = 6 per group). GAPDH was used as the loading control. Data were presented as mean ± SD. (B and E–G) One-way ANOVA with Bonferroni test; (C) One-way ANOVA with Bonferroni test or Student t-test; (D) Student's t test. *P < 0.05, **P < 0.01, ***P < 0.005, **** P < 0.001.

previously described[18] (see Supplementary material online, *Figure S3A*). Consequently, the proportion of Td^{+} cardiac RMs was significantly reduced in the heart of RM$^{TD\text{-}DTR}$ mice following DT treatment. Flow cytometry analyses further revealed that MaR1-induced reduction in total CD11b^{+}CD64^{+} macrophages after I/R injury was abolished in the hearts of DT-treated RM$^{TD\text{-}DTR}$ mice (*Figure 3A*). Notably, an increased number of TUNEL^{+} cells was observed in the DT-treated group following I/R injury, and MaR1 treatment failed to reduce the number of apoptotic cells in this context (*Figures 3B* and *S3B*). Echocardiogram analysis demonstrated that depletion of cardiac RMs markedly attenuated the MaR1-mediated improvement in cardiac function

Downloaded from academic.oup.com/cardiovascres/article/122/3/397/8430176 by Ewha Womans University Library - (INACTIVE) user on 28 August 2026

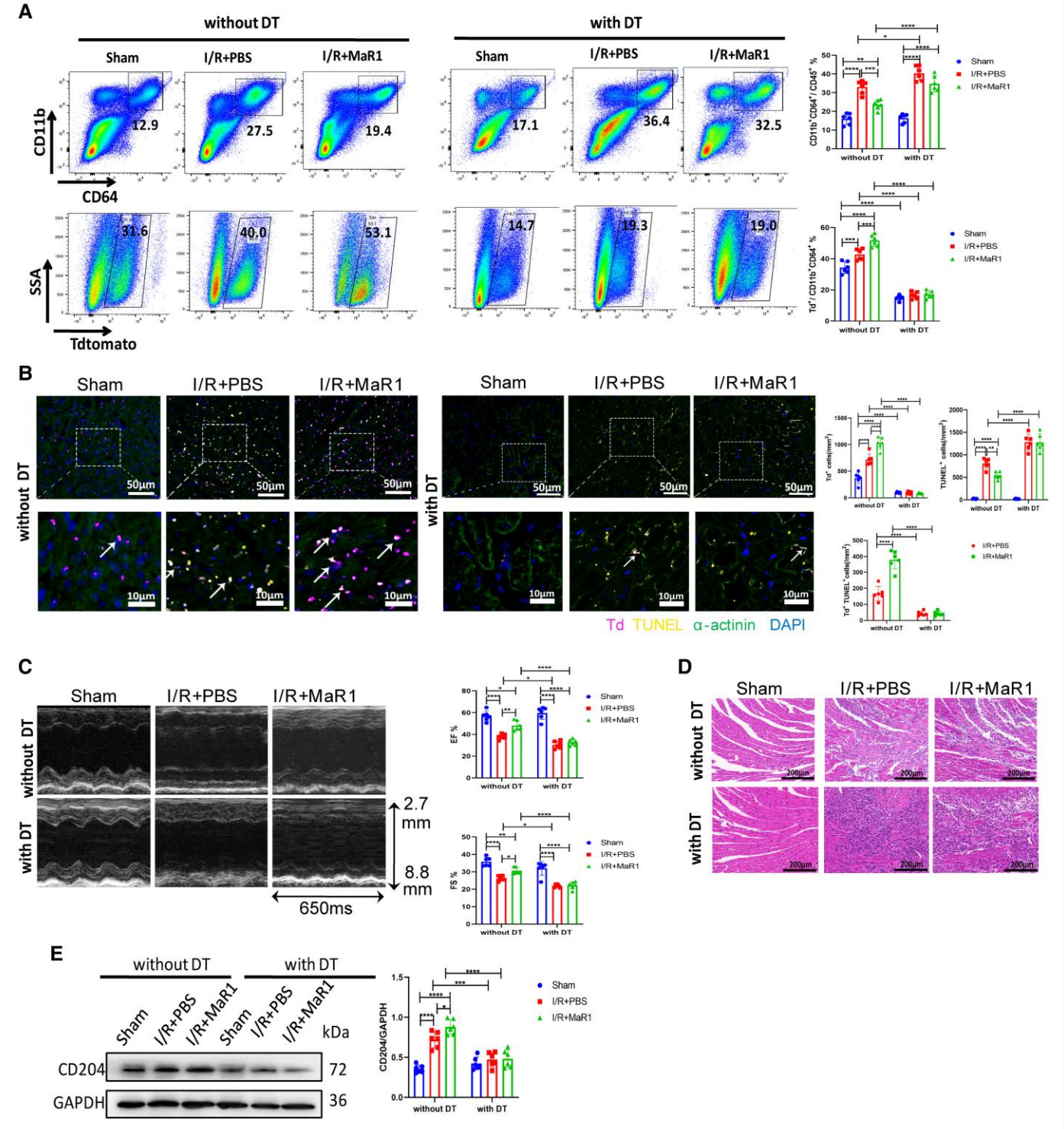


Figure 3 Conditional depletion of tissue resident macrophages abolishes the protective effect of MaR1. (*A*) Representative flow cytometry analyses and quantification of cardiac CD11b^{+} CD64^{+} Td^{+} macrophages from R26$^{Td\text{-}DTR}$ mice at day 3 after I/R (n = 6 per group). The number shown in gated region is the % for the representative sample. (*B*) Representative immunofluorescence images of Td^{+} cells (CX3CR1, pink) in cardiac sections stained with apoptotic cells (TUNEL, yellow), cardiac sarcomere (α-actinin, green) and nuclei (DAPI, blue) from R26$^{Td\text{-}DTR}$ mice at day 3 after I/R. Scale bar: upper = 50 μm; lower = 10 μm. Quantification of Td^{+} cells, TUNEL^{+} cells and Td^{+} TUNEL^{+} cells were shown on right (n = 6 per group). (*C*) Echocardiography measurements of cardiac function of R26$^{Td\text{-}DTR}$ mice. EF and FS were shown at day 3 after IR (n = 6 per group). (*D*) Representative images of HE staining of sequential cardiac sections from R26$^{Td\text{-}DTR}$ mice 3 days after I/R (n = 6 per group). Scale bar = 200μm. (*E*) Immunoblot analysis of CD204 in murine cardiac tissues at day 3 after I/R (n = 6 per group). GAPDH was used as the loading control. Data were presented as mean ± SD. (A–C and E) Two-way ANOVA followed by Bonferroni test. *P < 0.05, **P < 0.01, ***P < 0.005, **** P < 0.001.

Downloaded from academic.oup.com/cardiovascres/article/122/3/397/8430176 by Ewha Womans University Library - (INACTIVE) user on 28 August 2026

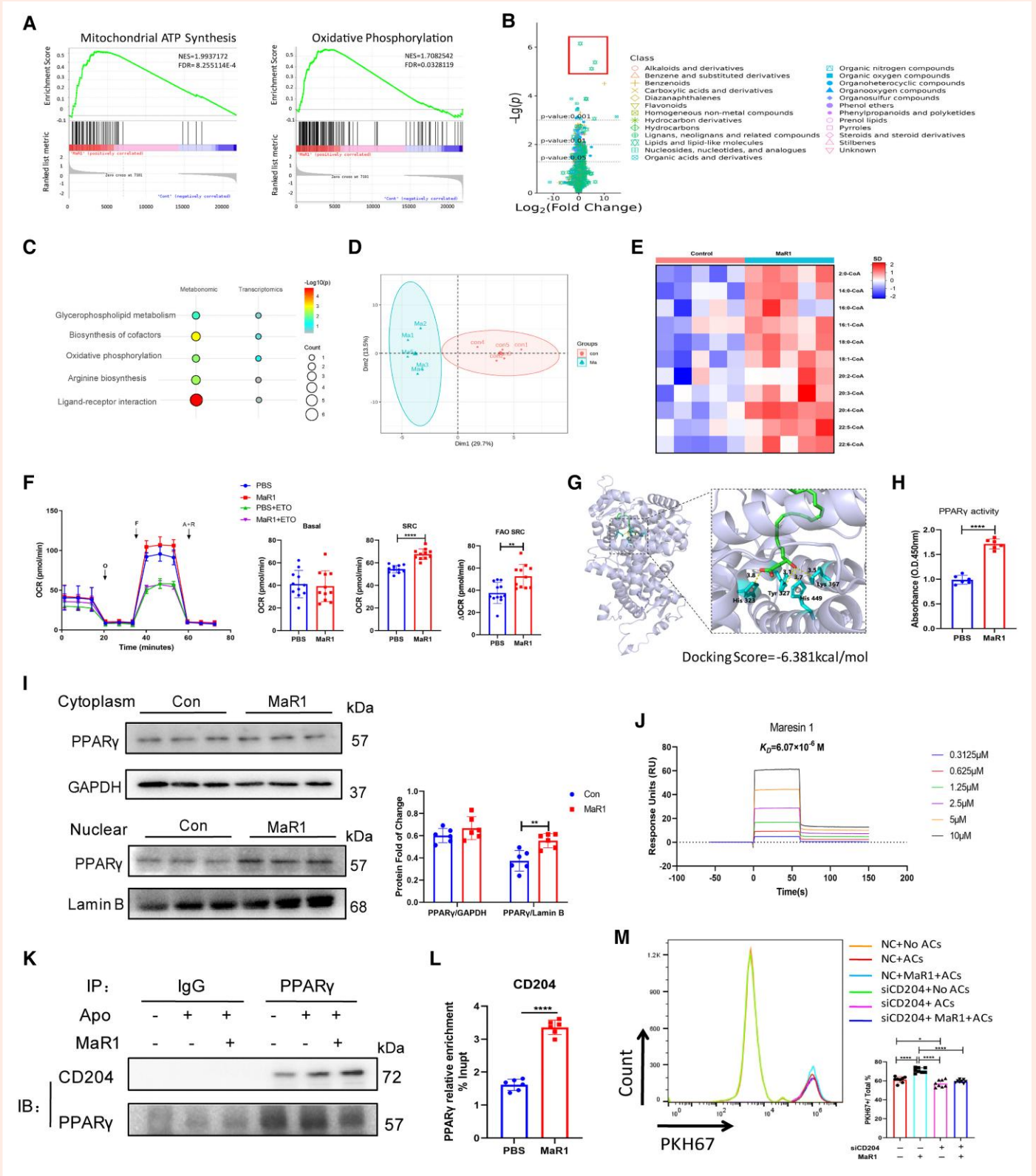


Figure 4 Fatty acid oxidation (FAO) is required for MaR1-mediated macrophage efferocytosis. *(A)* Gene set enrichment analysis (GSEA) from RNA sequencing data of metabolism-related genesets for mitochondrial ATP synthesis and the oxidative phosphorylation pathways. *(B)* Volcano plot from metabolome profiling classed by HMDB superclass in primary RMs (n = 3 per group). *(C)* The KEGG pathway at the intersection of RNA sequencing and metabolomic profiling in RMs. *(D)* Principal component analysis (PCA) of lipidomic data from RMs (n = 5 per group). *(E)* Heatmap produced from the lipidomic analysis in RMs (n = 5 per group). *(F)* FAO is identified by the measurement of the oxygen consumption rate (OCR) in RMs using a Seahorse XFp analyser. Cells were sequentially treated with oligomycin (O), FCCP (F) and antimycin A/rotenone (A + R). Etomoxir (ETO, an FAO inhibitor) was used to block the transport of fatty acids into the mitochondrion. The ΔOCR of basal

(continued)

Downloaded from academic.oup.com/cardiovascres/article/122/3/397/8430176 by Ewha Womans University Library - (INACTIVE) user on 28 August 2026

Figure 4 Continued
respiration and spare respiratory capacity (SRC) were calculated as the response of macrophages in the indicated groups to ETO treatment (n = 12 per group; t-test). *(G)* Molecular docking evaluation of MaR1 with PPARγ in a 3D schematic docked state. The docking score = −6.381 kcal/mol. *(H)* The detection of PPARγ transcriptional activity in RMs (n = 6 per group). *(I)* Immunoblot analysis of PPARγ in cytoplasm and nuclear from the primary sorted RMs (n = 6 replicates). *(J)* BIA core analysis for binding of MaR1 to PPARγ. The increasing concentrations of MaR1 were injected over immobilized PPARγ-His proteins on the sensor chip and K_D value was calculated by the BIA evaluation 3.1 software. *(K)* Cardiac RMs were incubated with apoptotic cells for 45 min after treatment with MaR1. The cell lysates were immunopurified with anti-PPARγ antibody. Then the expression of CD204 and PPARγ were measured by immunoblot. IgG was the negative control. *(L)* PPARγ occupancy of CD204 analysis in RMs after MaR1 treatment by ChIP-qPCR (n = 6 replicates). *(M)* Primary peritoneal macrophages were incubated with PKH67 labelled apoptotic cells (ACs) for 45 min after knockdown the CD204 expression. Unengulfed ACs were removed, the percentage of $PKH67^+$ cells among total macrophages was evaluated by flow cytometry shown in histograms (n = 8 replicates). Data were presented as mean ± SD. (F, H, and K) Student t-test; (I and M) one-way ANOVA with Bonferroni test. $^*P < 0.05$, $^{**}P < 0.01$, $^{***}P < 0.005$, $^{****}P < 0.001$.

(*Figure 3C*). Consistent with these findings, ablation of cardiac RMs substantially inhibited the MaR1-induced reduction in infarct size, activation of apoptosis signalling, inflammatory cell infiltration, and fibrosis within the myocardium (*Figures 3D* and *S3C–E*). Additionally, MaR1 treatment did not increase the expression of CD204 in cardiac tissues when RMs were depleted (*Figure 3E*). Collectively, these results indicate that the protective effects of MaR1 are dependent on cardiac RM efferocytosis in response to I/R injury.

3.5 The enhancement of PPARγ induced by MaR1 plays a critical role in promoting efferocytosis

To elucidate the anti-inflammatory mechanism of MaR1 in macrophages, we conducted RNA-sequencing (RNA-seq) analysis on primary RMs treated with MaR1. The results revealed that MaR1 significantly upregulated the expression of anti-inflammatory genes (Gpr18 and Mrc1) as well as angiogenesis-related genes (Pecam1 and Pgf) (see Supplementary material online, *Figure S4A*). Furthermore, the gene set enrichment analysis (GSEA) data revealed a marked increase in the mitochondrial ATP synthesis and oxidative phosphorylation (OXPHOS) signalling pathways upon MaR1 treatment (*Figure 4A*). The Kyoto encyclopaedia of genes and genomes (KEGG) enrichment analysis results revealed that MaR1 modulated both OXPHOS and arginine metabolism signalling pathways (see Supplementary material online, *Figure S4B*). Given that metabolic reprogramming is a key regulator of macrophage function, we performed metabolomic profiling to identify MaR1-mediated metabolic alterations in RMs. The HMDB superclass volcano plot highlighted significant changes in lipids and lipid-like molecules (*Figure 4B*). Notably, the levels of specific lipid molecules, including MaR1, 15,16-DiHODE, and carnitines, were elevated in the MaR1-treated group (see Supplementary material online, *Figure S4C* and *D*). We subsequently compared the results of the KEGG enrichment analyses of the RNA-seq and metabolomic data, revealing consistent enrichment of the glycerophospholipid metabolism, OXPHOS and arginine biosynthesis pathways following MaR1 treatment (*Figure 4C* and *S4E*). On the basis of these findings, we hypothesized that MaR1 influences the fatty acid oxidation (FAO) metabolism in cardiac RMs. To test this hypothesis, we conducted lipidomic analysis to assess lipid metabolic activity directly. Principal component analysis (PCA) and heatmap visualization confirmed that MaR1-treated RMs presented significantly higher levels of fatty acids than did the control group (*Figure 4D* and *E*). The mitochondrial oxygen consumption rate (OCR) and extracellular acidification rate (ECAR) were subsequently assessed using the Seahorse extracellular flux to evaluate the metabolic activity of RMs. An increase in OXPHOS and a decrease in glycolysis were observed in MaR1-treated RMs (see Supplementary material online, *Figure S4F*). FAO activity was measured by detecting OCR changes following treatment with ETO (an inhibitor of FAO). Additionally, the basal respiration rate and the spare respiratory capacity (SRC) change in OCR (ΔOCR) were determined to evaluate the impact of FAO on OXPHOS. The data demonstrated that MaR1 treatment increased FAO activity in RMs (*Figure 4F*). Furthermore, Q-PCR analysis of genes associated with metabolism corroborated these findings, indicating that MaR1 treatment increased the levels of FAO- and OXPHOS-related gene expression (see Supplementary material online, *Figure S4G*).

MaR1, a metabolic product of long-chain polyunsaturated fatty acids, is likely to serve as a natural ligand for the lipid-activated receptor superfamily in cardiac macrophages. Consequently, we investigated the effects of MaR1 on the expression of lipid nuclear receptors in RMs. Our data revealed that MaR1 treatment significantly upregulated the mRNA expression of PPARγ, whereas other receptors, including PPARα, PPARδ, retinoic acid–related orphan receptor (ROR), retinoid X receptor (RXR), and liver X receptor (LXR) remained unaffected (see Supplementary material online, *Figure S5A*). A docking structural model based on the conformation of MaR1 and PPARγ revealed that MaR1 was aptly accommodated within the ligand-binding site of PPARγ, facilitated by interactions with key residues His323, His449, Tyr327, and Lys367 (*Figure 4G*). We subsequently assessed the transcriptional activity of PPARγ. Compared with the RMs in the control group, the MaR1-treated RMs presented markedly increased PPARγ activation (*Figure 4H*). Consistently, the nuclear expression of PPARγ was significantly augmented by MaR1 (*Figure 4I*). Importantly, surface plasmon resonance (SPR) analysis confirmed the high binding affinity of MaR1 for the PPARγ protein (*Figure 4J*). To further validate the roles of PPARγ and FAO in MaR1-induced alterations in RMs, GW9662 (a selective PPARγ antagonist) and ETO were separately added to the RM culture medium. The increase in FAO and OXPHOS induced by MaR1 was abolished upon treatment with GW9662 or ETO (see Supplementary material online, *Figure S5B* and *C*). In addition, we found that GW9662 or ETO treatment suppressed the MaR1-mediated increase in efferocytosis (see Supplementary material online, *Figure S5D* and *E*). PPARγ activation contributes to the clearance of apoptotic cells by regulating the expression of efferocytosis receptors.[26] Therefore, we investigated the changes in efferocytosis receptor levels upon treatment. The transcription levels of Mertk, CD36, and CD204 were all reduced by GW9662 or ETO treatment, with CD204 showing the most significant decrease (see Supplementary material online, *Figure S5F*). We subsequently investigated whether MaR1 enhances CD204 transcription via PPARγ activation. Data from coimmunoprecipitation (co-IP) revealed that MaR1 treatment increased the interaction between CD204 and PPARγ (*Figure 4K*). Furthermore, chromatin immunoprecipitation (ChIP)-PCR experiments demonstrated increased enrichment of CD204 at the PPARγ promoter following MaR1 treatment (*Figure 4L*). To validate this mechanism, we

Downloaded from academic.oup.com/cardiovascres/article/122/3/397/8430176 by Ewha Womans University Library - (INACTIVE) user on 28 August 2026

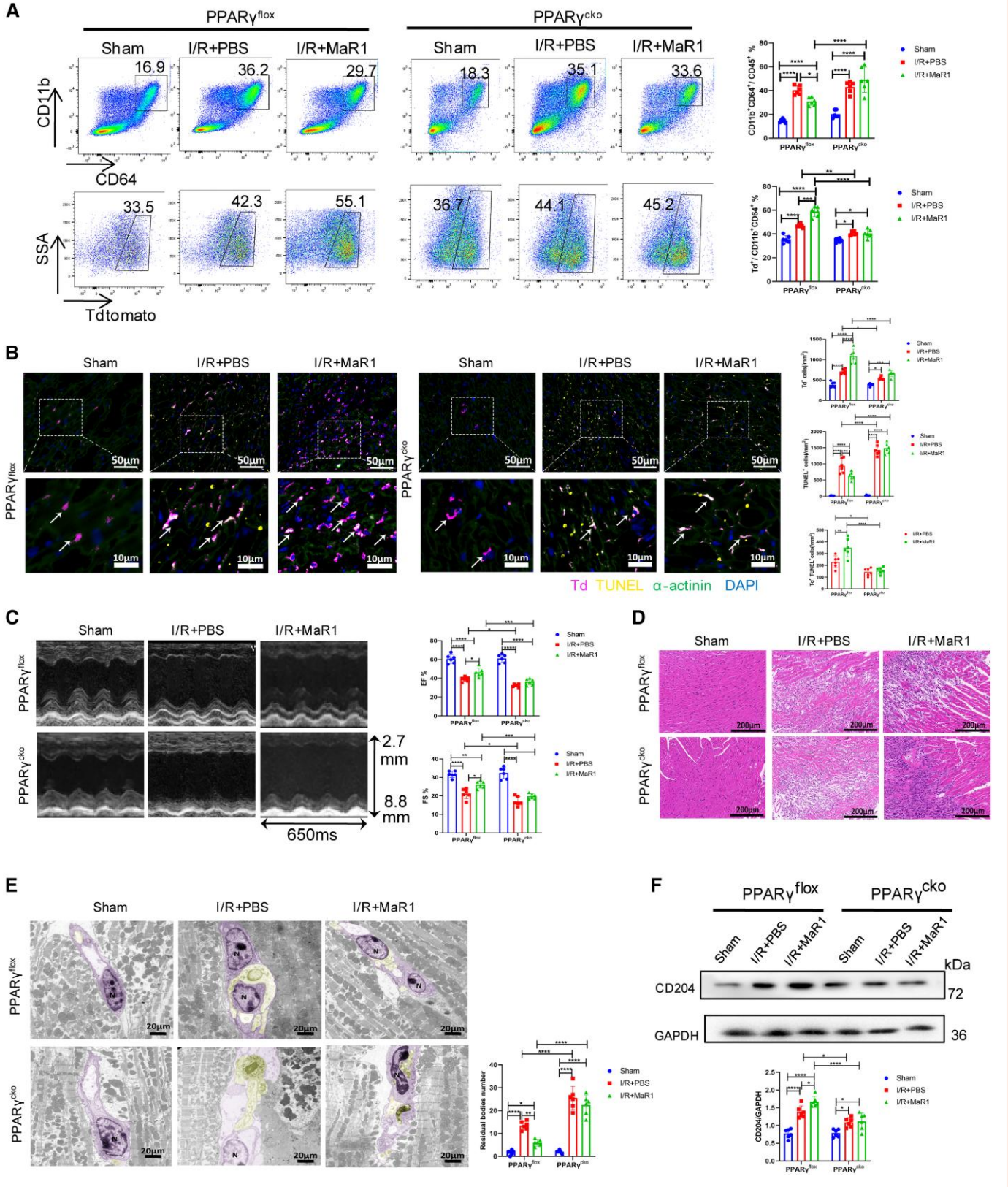


Figure 5 Inducible depletion of PPARγ in tissue resident macrophages attenuates MaR1 beneficial effect. (*A*) Representative flow cytometry analyses and quantification of cardiac CD11b$^+$ CD64$^+$ Td$^+$ macrophages from PPARγ^{flox} and PPARγ^{cko} mice at day 3 after I/R (n = 6 per group). The number shown in gated region is the % for the representative sample. (*B*) Representative immunofluorescence images of Td$^+$ cells (CX3CR1, pink) in cardiac sections stained with apoptotic cells (TUNEL, yellow), cardiac sarcomere (α-actinin, green) and nuclei (DAPI, blue) from PPARγ^{flox} and PPARγ^{cko} mice at day 3 after I/R. Scale bar: Upper = 50 μm; Lower = 10 μm. Quantification of Td + TUNEL + cells were

(continued)

Downloaded from academic.oup.com/cardiovascres/article/122/3/397/8430176 by Ewha Womans University Library - (INACTIVE) user on 28 August 2026

Figure 5 Continued
shown on right ($n = 6$ per group). *(C)* Echocardiography measurements of cardiac function of PPARγ^{flox} and PPARγ^{cko} mice. EF and FS were shown at day 3 after IR ($n = 6$ per group). *(D)* Representative images of HE staining of sequential cardiac sections from PPARγ^{flox} and PPARγ^{cko} mice treated with either MaR1 or PBS 3 days after I/R ($n = 6$ per group). Scale bar = 200 μm. *(E)* Representative TEM images of a macrophage (purple area) swallowing the debris in cardiac tissues at day 3 after I/R. Residual bodies can be identified by higher electrodensity (dark areas) in the phagocytic vesicles (yellow area). 'N' represents the cell nucleus. Scale bars =20μm. *(F)* Immunoblot analysis of CD204 expression in murine cardiac tissues at day 3 after I/R ($n = 6$ per group). GAPDH was used as the loading control. Data were presented as mean ± SD. (A–D) Two-way ANOVA followed by Bonferroni test. *$P < 0.05$, **$P < 0.01$, ***$P < 0.005$, **** $P < 0.001$.

silenced CD204 expression in macrophages using siRNA transfection (see Supplementary material online, *Figure S5G*), and selected sequence 1 of siCD204 for subsequent experiments. The flow cytometry data showed that CD204 knockdown attenuated macrophage efferocytosis even in the presence of MaR1 treatment (*Figure 4M*). Collectively, these findings suggest that MaR1 facilitates FAO by directly binding to PPARγ and enhances the transcription of its downstream receptor CD204, thereby promoting macrophage efferocytosis.

3.6 MaR1 improves myocardial I/R injury in a PPARγ-dependent manner

To further elucidate the role of PPARγ in MaR1-induced efferocytosis, cardiac RM specific PPARγ-deficient mice (PPARγ^{cko}) were generated by crossing PPARγ$^{fl/fl}$ mice with Cx3cr1$^{Td\text{-}creERT2}$ mice (see Supplementary material online, *Figure S6A*). The validity of this model was confirmed by detecting significantly reduced PPARγ protein levels in the cardiac RMs of PPARγ^{cko} mice (see Supplementary material online, *Figure S6B*). Flow cytometry data demonstrated that both the increase in Td$^+$ RMs and the decrease in total macrophages induced by MaR1 were abolished when PPARγ was depleted in cardiac RMs (*Figure 5A*). In addition, PPARγ deficiency in cardiac RMs markedly reversed the increase in efferocytosis and reduction in cell apoptosis mediated by MaR1 at 3 day post-I/R (*Figure 5B* and *S6C*). The improvement in cardiac function mediated by MaR1 was also attenuated in PPARγ^{cko} mice compared with the PPARγ$^{fl/fl}$ littermates (*Figure 5C*). Consistent with these findings, the suppression of inflammatory infiltration, infarct size, the apoptosis pathway and fibrosis in the myocardium of PPARγ$^{fl/fl}$ mice induced by MaR1 was significantly diminished in PPARγ^{cko} mice on day 3 post-I/R (*Figure 5D* and *S6D–F*). Importantly, specific ablation of PPARγ in cardiac RMs interrupted the digestion of residual bodies mediated by MaR1 during I/R injury (*Figure 5E*). Immunoblot analysis revealed that the expression of the efferocytosis receptor CD204 was also reduced in the cardiac tissues of PPARγ^{cko} mice following I/R (*Figure 5F*). Collectively, these data indicate that PPARγ in cardiac RM is essential for promoting MaR1-mediated efferocytosis, thereby fostering a proresolving milieu.

3.7 DHA improves I/R injury through its conversion into MaR1 in an Alox12-dependent manner

MaR1 is a well-characterized metabolite of DHA.[14,27] To investigate whether DHA treatment could mitigate I/R injury, the RM^{TD} mice were orally administered DHA for one week prior to I/R induction.[19] Our results demonstrated that EF and FS were significantly increased in the DHA-treated group than in the PBS-treated group following I/R injury (*Figure 6A*). Analysis of fatty acid metabolites showed that the levels of proresolving metabolites (MaR1, RvD1, and RvE1) were increased in the DHA-treated group than in the PBS-treated group post-I/R (see Supplementary material online, *Figure S7A*). Furthermore, DHA treatment reduced the infiltration of CD11b$^+$CD64$^+$ macrophages and enhanced the accumulation of Td$^+$ RMs in the hearts of I/R mice (*Figure 6B*). The infarct sizes in DHA-treated mice were markedly smaller than those in the PBS-treated mice following I/R injury (*Figure 6C*). Additionally, the DHA-treated mice exhibited reduced inflammatory cell recruitment, attenuated fibrosis, and decreased apoptosis in the myocardium (see Supplementary material online, *Figure S7B* and *C*). TUNEL staining revealed a decreased number of apoptotic cells and an increased number of Td$^+$TUNEL$^+$ cells in DHA-treated mice, indicating improved efferocytosis by cardiac RMs (*Figure 6D*). Moreover, the protein levels of PPARγ and CD204 were increased after DHA treatment, supporting the translational activation of PPARγ by DHA (*Figure 6E*).

Although both our studies and those of others conducted on animal models demonstrated the protective effect of DHA against I/R injury,[28,29] large clinical studies have reported conflicting findings, causing confusion among the public and health professionals.[30] In recent clinical trials, treatment with EPA monotherapy has demonstrated superior efficacy in reducing cardiovascular events compared with mixed EPA/DHA formulations.[31,32] To elucidate the distinct mechanisms of action of DHA and EPA, we investigated their metabolic pathways. As depicted in *Figure 6F*, EPA and DHA are metabolized to produce a variety of bioactive lipid mediators through the action of different lipoxygenases (LOXs). Therefore, we analysed the gene expression of LOXs involved in the metabolism of EPA and DHA in cardiac tissues from patients with ischaemic heart diseases using transcriptome analysis (GSE57338). Our results revealed that the expression levels of the 12-LOX encoding gene *Alox12* and the 5-LOX encoding gene *Alox5* were significantly lower in the heart failure group than in the non-failing group (*Figures 6G* and *S7D*). Given that 12-LOX is the exclusive metabolic enzyme responsible for the conversion of DHA into MaR1, we hypothesized that the downregulation of *Alox12* might impact the protective effects of DHA. To test this hypothesis, we constructed a heart-specific cTNT promoter-driven adeno-associated virus (AAV9) encoding *Alox12*. Following 21 days of transfection in RM^{Td} mice, the protein levels of Alox12 in the hearts of the mice were examined (see Supplementary material online, *Figure S7E*). Of note, Alox12 knockdown prevented DHA-mediated improvement in cardiac function following I/R injury at day 3 (*Figure 6H*). Flow cytometry analyses further indicated that Alox12 inhibition led to an increase in total macrophages and a decrease in Td$^+$ RMs within the myocardium (*Figure 6I*). Moreover, the ablation of Alox12 reversed the protective effects of DHA treatment, including reducing infarction size, decreasing inflammation infiltration and reducing fibrosis (*Figure 6J* and *S7F*). Collectively, these findings suggest that DHA may exert its cardioprotective effects by decomposing into MaR1 in an Alox12-dependent manner.

4. Discussion

The acute inflammatory cascade response is responsible for the onset and progression of myocardial I/R injury. Given that cardiac RMs are important contributors to cardiac inflammation and repair, immunomodulatory strategies targeting cardiac RMs could

Downloaded from academic.oup.com/cardiovascres/article/122/3/397/8430176 by Ewha Womans University Library - (INACTIVE) user on 28 August 2026

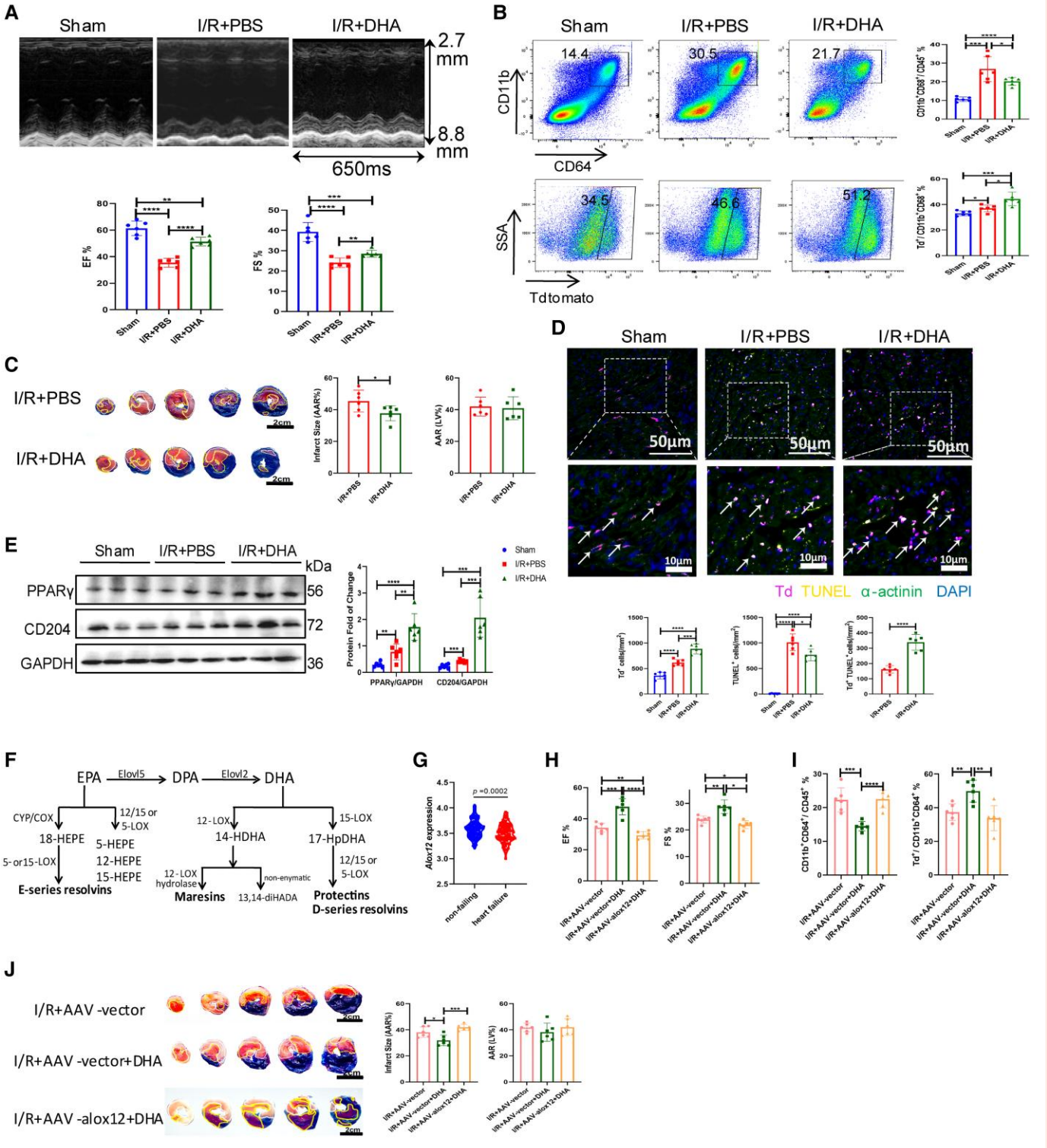


Figure 6 DHA, a precursor drug to MaR1, could attenuate I/R injury. *(A)* Echocardiography measurements of cardiac function of RM^{Td} mice. EF and FS were shown at day 3 after IR ($n = 6$ per group). *(B)* Representative flow cytometry analyses and quantification of cardiac $CD11b^+$ $CD64^+$ Td^+ macrophages from RM^{Td} mice at day 3 after I/R or sham operation ($n = 6$ per group). The number shown in gated region is the % for the representative sample. *(C)* Representative images of Evans blue and TTC double-stained sequential cardiac sections from mice. Scale bar = 2 cm. Quantitative analyses of the percentage AAR and infarct size are shown ($n = 6$ per group). *(D)* Representative immunofluorescence images of Td^+ cells (CX3CR1, pink) in cardiac sections stained with apoptotic cells (TUNEL, yellow), cardiac sarcomere (α-actinin, green) and nuclei (DAPI, blue) from RM^{Td} mice at day 3 after I/R. Scale bar: Upper = 50 μm; Lower = 10 μm. Quantification of Td^+ cells, $TUNEL^+$ cells and Td^+ $TUNEL^+$ cells were shown below ($n = 6$ per group). *(E)* Immunoblot analysis of PPARγ and CD204 in murine cardiac tissues at day 3 after I/R ($n = 6$ per group). GAPDH was used as the loading control. *(F)* A scheme for metabolic process of EPA and DHA by LOX family.

(continued)

Downloaded from academic.oup.com/cardiovascres/article/122/3/397/8430176 by Ewha Womans University Library - (INACTIVE) user on 28 August 2026

Figure 6 Continued
(G) Reanalysis of alox12 gene expression in left ventricle tissues from GEO data set GSE57338 (136 nonfailing donors and 95 ischaemic heart disease donors). *(H)* Echocardiography measurements of cardiac function of RM^{Td} mice after AAV transfection following I/R injury. EF and FS were shown (n = 6 per group). *(I)* Flow cytometry analyses and quantification of cardiac $CD11b^+$ $CD64^+$ Td^+ macrophages from RM^{Td} mice after AAV transfection following I/R injury (n = 6 per group). *(J)* Representative images of Evans blue and TTC double-stained sequential cardiac sections from mice. Scale bar = 2 cm. Quantitative analyses of the percentage AAR and infarct size are shown (n = 6 per group). Data were presented as mean ± SD. (A–C, E–F, and I–K) One-way ANOVA with Bonferroni test; (D and H) Student t-test. $^*P < 0.05$, $^{**}P < 0.01$, $^{***}P < 0.005$, $^{****}P < 0.001$.

potentially enhance the intrinsic capacity for inflammation resolution. MaR1, a lipid mediator of the SPM family, resolves inflammation by reducing neutrophil trafficking and promoting macrophage phagocytosis. However, the role of MaR1 in regulating the metabolic transition of cardiac macrophages following myocardial I/R injury remains unclear. In this study, we found that MaR1 levels were negatively associated with inflammation and the severity of I/R injury in STEMI patients. Administration of MaR1 enhanced efferocytosis in cardiac RMs by increasing the transcriptional activity of PPARγ on the scavenger receptor CD204, thereby mitigating the inflammatory response and reducing cardiac damage. Additionally, DHA, a precursor of MaR1, exhibited therapeutic potential in mitigating the progression of I/R injury. Together, these findings increase our understanding of how MaR1 regulates macrophage metabolism and offer potential targets for treating myocardial I/R injury.

Cardiac RMs are generally recognized as the first-line responders to myocardial damage.[33] Previous studies have demonstrated that cardiac stem therapy confers cardiac benefits through the induction of RMs,[34] highlighting the intrinsic wound healing microenvironment supported by RMs. Consistent with these findings, our data revealed that cardiac RMs exhibit rapid responsiveness to MaR1 administration, enhancing their phagocytic activity and promoting cardiac repair (*Figures 1* and *2*). Deletion of cardiac RMs significantly diminished the efficacy of MaR1 in attenuating inflammation and preserving cardiac function (*Figure 3*). These findings suggest that strategies focused on the application of MaR1 to restrain excessive inflammation and myocardial injury should also aim to preserve cardiac RM, thereby optimizing cardiac repair.

Previous work has shown that efferocytosis promotes mitochondrial homeostasis and metabolic bias,[12,35] leading to various metabolic adaptations in macrophages that facilitate tissue resolution.[36] Our data suggested that the clearance of apoptotic cells by MaR1-treated macrophages is associated with significant enhancements in OXPHOS and FAO (*Figure 4*), suggesting that MaR1 may strengthen these pathways and contribute to metabolic alterations in macrophages. Similarly, Hosseini et al. reported increased FAO and OXPHOS in macrophages treated with RvD1 during atherosclerosis.[37] Moreover, FAO plays a critical role in sustaining the energy demands of continuous efferocytosis.[12] Thus, treatment with MaR1 and other SPM lipid mediators can support sustained resolution during inflammatory responses.

As a stereoselective lipid, MaR1 has a localized anti-inflammatory effect through binding to distinct receptors in various tissues. It has been reported that leucine-rich repeat domain-containing G protein-coupled receptor 6 (LGR6) mediates the phagocyte immunoresolvent functions of MaR1.[38] Additional reports have demonstrated that MaR1 directly interacts with the retinoic acid–related orphan receptor a (RORa) in liver macrophages.[16] Besides, Qiu et al. demonstrated that MaR1 increased the nuclear translocation of Nrf2 in renal I/R injury.[39] PPARγ plays a critical role in lipid metabolism, including transportation, phospholipid production and the handling of inflammation.[40] Our results showed that MaR1 significantly increased the transcriptional activity of PPARγ. SPR analysis confirmed the high binding affinity of MaR1 for the PPARγ protein (*Figure 4*). Moreover, cardiac RM-specific knockout of PPARγ abrogated the proresolving effects mediated by MaR1 (*Figure 5*). Given that ligands often interact with multiple receptors, these results suggest that MaR1 exhibits diverse modes of action depending on the context. Given that LGR6 exhibits a better affinity for drugs than PPARγ, another possibility that cannot be excluded is that MaR1 binds to the LGR6 receptor on the membrane surface, triggering downstream signalling pathways that subsequently activate intracellular PPARγ, which warrants further investigation.

Although the myeloid-epithelial-reproductive protein tyrosine kinase (Mertk) receptor is recognized as a classical efferocytosis receptor of macrophages,[8] we did not observe a significant alteration in Mertk expression following MaR1 treatment. This lack of change may be attributed to the proteolytic cleavage of Mertk on cardiac RMs during the I/R.[7] Our data demonstrated that MaR1 significantly increased the expression of CD204 on cardiac RMs (*Figure 4*). CD204, also known as scavenger receptor A1 (SR-A1), functions acts as a phagocytic receptor in macrophages and is involved in the uptake of modified lipoproteins, debris and apoptotic cells.[25] In addition, our previous study has demonstrated that CD204 can alleviate inflammatory cardiomyopathy by modulating the activity of cardiac RMs.[17] Notably, the present study revealed that MaR1 enhanced the interaction between PPARγ and CD204, thereby facilitating PPARγ-mediated transcriptional regulation of CD204 (*Figure 4*). The phagocytic activity of macrophages was reduced upon blockade of CD204, and even the addition of MaR1 failed to restore this activity. Taken together, these data support the notion that MaR1-mediated activation of PPARγ upregulates CD204 expression, thereby accelerating the clearance of apoptotic cells and resolving inflammation following I/R injury.

MaR1 is derived from DHA during inflammation response. It is reported that MaR1 peaks 4 h post-pathogens challenge and declines to baseline by 24 hour.[41] In an ideal situation, the stimuli are resolved, and the tissue will gradually return to homeostasis. If this inflammation progress is not controlled, chronic inflammatory diseases will evolve. Persistently low MaR1 levels in diseases reflect impaired inflammation resolution, thus regarding it as a biomarker.[42–44] Our results also demonstrated that the plasma levels of MaR1 were associated with inflammation and the severity of I/R injury in STEMI patients (*Figure 1*). Consistently, the levels of ω-3 PUFAs are associated with the risk of cardiovascular disease.[30] Thus, MaR1's dynamic turnover provides a physiological readout of resolution status.

Treatment with ω-3 PUFA supplements containing EPA and DHA for primary and secondary prevention have reported conflicting findings.[45] This may be attributed to two reasons. First, the bioavailability of ω-3 PUFAs is different across populations. Our results demonstrated that the expression of the MaR1 biosynthetic enzyme, *Alox12*, was reduced in the cardiac tissues of ischaemic cardiomyopathy patients (*Figure 6*). Although daily oral administration of DHA improved myocardial I/R injury in mice, knocking down the expression of *Alox12* reversed the protective effect of DHA (*Figure 6*). These data suggest that MaR1 biosynthetic pathways may be interrupted by cardiac damage, consistent with studies reporting defective SPM synthesis in human atherosclerotic

Downloaded from academic.oup.com/cardiovascres/article/122/3/397/8430176 by Ewha Womans University Library - (INACTIVE) user on 28 August 2026

plaques.[46,47] Essential fatty acids might not be efficiently converted into bioactive mediators in patients, and supplementation with high-purity SPM mediators could provide greater cardiovascular benefits. Second, the MaR1 and other SPMs are susceptible to metabolic inactivation upon entering the circulation. It is reported that MaR1 is synthesized locally and functions locally, and is subsequently converted to 14-oxoMaR1, resulting in loss of bioactivity.[48] A randomized, double-blind, placebo-controlled trial demonstrated that plasma levels of MaR1 peak within 4 h following oral fish oil administration and decrease significantly by 6 h, indicating its rapid metabolism in the circulation.[49] This metabolic lability is consistent with other SPMs.[50,51] Thus, intramyocardial injection was employed in this study to preserve its activity (*Figure 1–4*). However, this approach deviates from standard clinical practices. Nanoparticles enable targeted and stable delivery of therapeutic compounds, offering promising opportunities for the intravenous administration of MaR1. Notably, nano-based therapeutics is increasingly being adopted in clinical settings or is under active investigation in clinical trials.[52] Therefore, the future development of nanomedicines for the delivery of MaR1 and other SPMs holds great potential for treating myocardial I/R injury.

However, the current study has the following limitations. The number of STEMI patients enrolled in the study was not sufficient, and no follow-up investigations were conducted. Although the RM^{Td} strain is highly efficient at manipulating cardiac RMs, it lacks a specific marker for these cells. The exclusive indicators of cardiac RMs need to be further explored. In addition, the exclusive use of male mice represents a methodological constraint. Lastly, although this study demonstrated the cardioprotective effects of MaR1 in the myocardial I/R injury, further investigations involving large animals and primates are necessary to fully evaluate the efficacy and safety of these potential therapeutic agents.

5. Conclusions

In summary, our study reveals the critical role of MaR1 in resolving inflammation and promoting cardiac repair through the regulation of efferocytosis by cardiac RMs, and identifies a promising therapeutic target for managing I/R injury.

Supplementary material

Supplementary material is available at *Cardiovascular Research* online.

Authors' contributions

X.S. and Y.F. participated in the study design and performed the in vitro experiments, analysed the data, and drafted the manuscript. X.S., Y.Z., Y.C., and Z.C. designed and performed the in vivo mouse experiments and analysed data. Y.Z. and A.D. collected the human blood samples and provided clinical data. X.S. and Z.W. evaluated and analysed the clinical data. B.X. revised the manuscript and provided professional advice. All the authors read and approved the final manuscript.

Acknowledgements

All the coauthors read and approved the final manuscript. The authors are grateful to Prof. Qi Chen (Department of Pathophysiology, Nanjing Medical University) for scientific advice; we also thank Ruoyu Dang (Tianjin Medical University) and Shaojun Wu (Department of Cardiology, Nanjing Drum Tower Hospital) for consulting on the results of the molecule docking experiments.

Conflict of interest: none declared.

Funding

The work was supported by the Key Research and Development Plan of the National Natural Science Foundation of China (grant number 2022YFA1205904), the Natural Science Foundation of China (grant number 82100525), the Jiangsu Natural Science Foundation (grant number BK20210013), and the Science Technology Foundation for Distinguished Young Scholars of Nanjing (grant number JQX23004).

References

1. Algoet M, Janssens S, Himmelreich U, Gsell W, Pusovnik M, Van den Eynde J, Oosterlinck W. Myocardial ischemia-reperfusion injury and the influence of inflammation. *Trends Cardiovasc Med* 2023;**33**:357–366.
2. Chen R, Zhang H, Tang B, Luo Y, Yang Y, Zhong X, Chen S, Xu X, Huang S, Liu C. Macrophages in cardiovascular diseases: molecular mechanisms and therapeutic targets. *Signal Transduct Target Ther* 2024;**9**:130.
3. Zhuang L, Zong X, Yang Q, Fan Q, Tao R. Interleukin-34-NF-kappaB signaling aggravates myocardial ischemic/reperfusion injury by facilitating macrophage recruitment and polarization. *EBioMedicine* 2023;**95**:104744.
4. Ma Y, Mouton AJ, Lindsey ML. Cardiac macrophage biology in the steady-state heart, the aging heart, and following myocardial infarction. *Transl Res* 2018;**191**:15–28.
5. Dick SA, Macklin JA, Nejat S, Momen A, Clemente-Casares X, Althagafi MG, Chen J, Kantores C, Hosseinzadeh S, Aronoff L, Wong A, Zaman R, Barbu I, Besla R, Lavine KJ, Razani B, Ginhoux F, Husain M, Cybulsky MI, Robbins CS, Epelman S. Self-renewing resident cardiac macrophages limit adverse remodeling following myocardial infarction. *Nat Immunol* 2019;**20**:29–39.
6. Wong NR, Mohan J, Kopecky BJ, Guo S, Du L, Leid J, Feng G, Lokshina I, Dmytrenko O, Luehmann H, Bajpai G, Ewald L, Bell L, Patel N, Bredemeyer A, Weinheimer CJ, Nigro JM, Kovacs A, Morimoto S, Bayguinov PO, Fisher MR, Stump WT, Greenberg M, Fitzpatrick JAJ, Epelman S, Kreisel D, Sah R, Liu Y, Hu H, Lavine KJ. Resident cardiac macrophages mediate adaptive myocardial remodeling. *Immunity* 2021;**54**:2072–2088.e7.
7. DeBerge M, Yeap XY, Dehn S, Zhang S, Grigoryeva L, Misener S, Procissi D, Zhou X, Lee DC, Muller WA, Luo X, Rothlin C, Tabas I, Thorp EB. MerTK cleavage on resident cardiac macrophages compromises repair after myocardial ischemia reperfusion injury. *Circ Res* 2017;**121**:930–940.
8. Wan E, Yeap XY, Dehn S, Terry R, Novak M, Zhang S, Iwata S, Han X, Homma S, Drosatos K, Lomasney J, Engman DM, Miller SD, Vaughan DE, Morrow JP, Kishore R, Thorp EB. Enhanced efferocytosis of apoptotic cardiomyocytes through myeloid-epithelial-reproductive tyrosine kinase links acute inflammation resolution to cardiac repair after infarction. *Circ Res* 2013;**113**:1004–1012.
9. Bajpai G, Schneider C, Wong N, Bredemeyer A, Hulsmans M, Nahrendorf M, Epelman S, Kreisel D, Liu Y, Itoh A, Shankar TS, Selzman CH, Drakos SG, Lavine KJ. The human heart contains distinct macrophage subsets with divergent origins and functions. *Nat Med* 2018;**24**:1234–1245.
10. Pietrangelo A, Ouimet M. Death eaters rely on metabolic signaling to wield anti-inflammatory responses. *Cell Metab* 2019;**29**:234–236.
11. Doran AC, Yurdagul A Jr, Tabas I. Efferocytosis in health and disease. *Nat Rev Immunol* 2020;**20**:254–267.
12. Zhang S, Weinberg S, DeBerge M, Gainullina A, Schipma M, Kinchen JM, Ben-Sahra I, Gius DR, Yvan-Charvet L, Chandel NS, Schumacker PT, Thorp EB. Efferocytosis fuels requirements of fatty acid oxidation and the electron transport chain to polarize macrophages for tissue repair. *Cell Metab* 2019;**29**:443–456.e5.
13. Halade GV, Kain V, De La Rosa X, Lindsey ML. Metabolic transformation of fat in obesity determines the inflammation resolving capacity of splenocardiac and cardiorenal networks in heart failure. *Am J Physiol Heart Circ Physiol* 2022;**322**:H953–H970.
14. Serhan CN, Levy BD. Resolvins in inflammation: emergence of the pro-resolving superfamily of mediators. *J Clin Invest* 2018;**128**:2657–2669.
15. Dalli J, Serhan CN. Identification and structure elucidation of the pro-resolving mediators provides novel leads for resolution pharmacology. *Br J Pharmacol* 2019;**176**:1024–1037.
16. Han YH, Shin KO, Kim JY, Khadka DB, Kim HJ, Lee YM, Cho WJ, Cha JY, Lee BJ, Lee MO. A maresin 1/RORalpha/12-lipoxygenase autoregulatory circuit prevents inflammation and progression of nonalcoholic steatohepatitis. *J Clin Invest* 2019;**129**:1684–1698.
17. Zhang H, Xu A, Sun X, Yang Y, Zhang L, Bai H, Ben J, Zhu X, Li X, Yang Q, Wang Z, Wu W, Yang D, Zhang Y, Xu Y, Chen Q. Self-maintenance of cardiac resident reparative macrophages attenuates doxorubicin-induced cardiomyopathy through the SR-A1-c-Myc axis. *Circ Res* 2020;**127**:610–627.
18. Parkhurst CN, Yang G, Ninan I, Savas JN, Yates JR 3rd, Lafaille JJ, Hempstead BL, Littman DR, Gan WB. Microglia promote learning-dependent synapse formation through brain-derived neurotrophic factor. *Cell* 2013;**155**:1596–1609.

Downloaded from academic.oup.com/cardiovascres/article/122/3/397/8430176 by Ewha Womans University Library - (INACTIVE) user on 28 August 2026

19. Fan G, Li Y, Chen J, Zong Y, Yang X. DHA/AA alleviates LPS-induced kupffer cells pyroptosis via GPR120 interaction with NLRP3 to inhibit inflammasome complexes assembly. *Cell Death Dis* 2021;**12**:73.
20. Zaman R, Hamidzada H, Kantores C, Wong A, Dick SA, Wang Y, Momen A, Aronoff L, Lin J, Razani B, Mital S, Billia F, Lavine KJ, Nejat S, Epelman S. Selective loss of resident macrophage-derived insulin-like growth factor-1 abolishes adaptive cardiac growth to stress. *Immunity* 2021;**54**:2057–2071.e6.
21. Panigrahy D, Gilligan MM, Serhan CN, Kashfi K. Resolution of inflammation: an organizing principle in biology and medicine. *Pharmacol Ther* 2021;**227**:107879.
22. Yurdagul A Jr, Subramanian M, Wang X, Crown SB, Ilkayeva OR, Darville L, Kolluru GK, Rymond CC, Gerlach BD, Zheng Z, Kuriakose G, Kevil CG, Koomen JM, Cleveland JL, Muoio DM, Tabas I. Macrophage metabolism of apoptotic cell-derived arginine promotes continual efferocytosis and resolution of injury. *Cell Metab* 2020;**31**:518–533.e10.
23. DeBerge M, Glinton K, Subramanian M, Wilsbacher LD, Rothlin CV, Tabas I, Thorp EB. Macrophage AXL receptor tyrosine kinase inflames the heart after reperfused myocardial infarction. *J Clin Invest* 2021;**131**:e139576.
24. Luo Z, Sheng Z, Hu L, Shi L, Tian Y, Zhao X, Yang W, Xiao Z, Shen D, Wu W, Lan T, Zhao B, Wang X, Zhuang N, Zhang JN, Wang Y, Lu Y, Wang L, Zhang C, Wang P, An J, Yang F, Li Q. Targeted macrophage phagocytosis by Irg1/itaconate axis improves the prognosis of intracerebral hemorrhagic stroke and peritonitis. *EBioMedicine* 2024;**101**:104993.
25. Shichita T, Ito M, Morita R, Komai K, Noguchi Y, Ooboshi H, Koshida R, Takahashi S, Kodama T, Yoshimura A. MAFB prevents excess inflammation after ischemic stroke by accelerating clearance of damage signals through MSR1. *Nat Med* 2017;**23**:723–732.
26. Roszer T. Transcriptional control of apoptotic cell clearance by macrophage nuclear receptors. *Apoptosis* 2017;**22**:284–294.
27. Serhan CN. Pro-resolving lipid mediators are leads for resolution physiology. *Nature* 2014;**510**:92–101.
28. Wang CP, Lee CC, Wu DY, Chen SY, Lee TM. Differential effects of EPA and DHA on PPARgamma-mediated sympathetic innervation in infarcted rat hearts by GPR120-dependent and -independent mechanisms. *J Nutr Biochem* 2022;**103**:108950.
29. Madingou N, Gilbert K, Tomaro L, Prud'homme Touchette C, Trudeau F, Fortin S, Rousseau G. Comparison of the effects of EPA and DHA alone or in combination in a murine model of myocardial infarction. *Prostaglandins Leukot Essent Fatty Acids* 2016;**111**:11–16.
30. Sherratt SCR, Mason RP, Libby P, Steg PG, Bhatt DL. Do patients benefit from omega-3 fatty acids? *Cardiovasc Res* 2024;**119**:2884–2901.
31. Siscovick DS, Barringer TA, Fretts AM, Wu JH, Lichtenstein AH, Costello RB, Kris-Etherton PM, Jacobson TA, Engler MB, Alger HM, Appel LJ, Mozaffarian D; American Heart Association Nutrition Committee of the Council on Lifestyle and Cardiometabolic Health; Council on Epidemiology and Prevention; Council on Cardiovascular Disease in the Young; Council on Cardiovascular and Stroke Nursing; and Council on Clinical Cardiology. Omega-3 polyunsaturated fatty acid (fish oil) supplementation and the prevention of clinical cardiovascular disease: a science advisory from the American Heart Association. *Circulation* 2017;**135**:e867–e884.
32. Yokoyama M, Origasa H, Matsuzaki M, Matsuzawa Y, Saito Y, Ishikawa Y, Oikawa S, Sasaki J, Hishida H, Itakura H, Kita T, Kitabatake A, Nakaya N, Sakata T, Shimada K, Shirato K; Japan EPA lipid intervention study (JELIS) Investigators. Effects of eicosapentaenoic acid on major coronary events in hypercholesterolaemic patients (JELIS): a randomised open-label, blinded endpoint analysis. *Lancet* 2007;**369**:1090–1098.
33. Yap J, Irei J, Lozano-Gerona J, Vanapruks S, Bishop T, Boisvert WA. Macrophages in cardiac remodelling after myocardial infarction. *Nat Rev Cardiol* 2023;**20**:373–385.
34. Vagnozzi RJ, Maillet M, Sargent MA, Khalil H, Johansen AKZ, Schwanekamp JA, York AJ, Huang V, Nahrendorf M, Sadayappan S, Molkentin JD. An acute immune response underlies the benefit of cardiac stem cell therapy. *Nature* 2020;**577**:405–409.
35. Wang Y, Subramanian M, Yurdagul A Jr, Barbosa-Lorenzi VC, Cai B, de Juan-Sanz J, Ryan TA, Nomura M, Maxfield FR, Tabas I. Mitochondrial fission promotes the continued clearance of apoptotic cells by macrophages. *Cell* 2017;**171**:331–345.e22.
36. Schilperoort M, Ngai D, Sukka SR, Avrampou K, Shi H, Tabas I. The role of efferocytosis-fueled macrophage metabolism in the resolution of inflammation. *Immunol Rev* 2023;**319**:65–80.
37. Hosseini Z, Marinello M, Decker C, Sansbury BE, Sadhu S, Gerlach BD, Bossardi Ramos R, Adam AP, Spite M, Fredman G. Resolvin D1 enhances necroptotic cell clearance through promoting macrophage fatty acid oxidation and oxidative phosphorylation. *Arterioscler Thromb Vasc Biol* 2021;**41**:1062–1075.
38. Chiang N, Libreros S, Norris PC, de la Rosa X, Serhan CN. Maresin 1 activates LGR6 receptor promoting phagocyte immunoresolvent functions. *J Clin Invest* 2023;**133**:e168084.
39. Qiu Y, Wu Y, Zhao H, Sun H, Gao S. Maresin 1 mitigates renal ischemia/reperfusion injury in mice via inhibition of the TLR4/MAPK/NF-kappaB pathways and activation of the Nrf2 pathway. *Drug Des Devel Ther* 2019;**13**:739–745.
40. Montaigne D, Butruille L, Staels B. PPAR control of metabolism and cardiovascular functions. *Nat Rev Cardiol* 2021;**18**:809–823.
41. Serhan CN, Yang R, Martinod K, Kasuga K, Pillai PS, Porter TF, Oh SF, Spite M. Maresins: novel macrophage mediators with potent antiinflammatory and proresolving actions. *J Exp Med* 2009;**206**:15–23.
42. Oliveira Perucci L, Pereira Santos TA, Campi Santos P, Ribeiro Teixeira LC, Nessralla Alpoim P, Braga Gomes K, Pires Sousa L, Sant'Ana Dusse LM, Talvani A. Pre-eclampsia is associated with reduced resolvin D1 and maresin 1 to leukotriene B4 ratios in the plasma. *Am J Reprod Immunol* 2020;**83**:e13206.
43. Li M, Sun Y, Liu B, Xue Y, Zhu M, Zhang K, Jing Y, Ding H, Liang Y, Zhou H, Dong C. Association between plasma maresin 1 and the risk of atherosclerotic cardiovascular disease in Chinese adults: a community-based cohort study. *Nutr Metab Cardiovasc Dis* 2024;**34**:1631–1638.
44. Demirci S, Sezer S. Serum Maresin-1 and Resolvin-D1 levels as non-invasive biomarkers for monitoring disease activity in ulcerative colitis. *Diagnostics* 2025;**15**:834.
45. Aung T, Halsey J, Kromhout D, Gerstein HC, Marchioli R, Tavazzi L, Geleijnse JM, Rauch B, Ness A, Galan P, Chew EY, Bosch J, Collins R, Lewington S, Armitage J, Clarke R; Omega-3 Treatment Trialists' Collaboration. Associations of Omega-3 fatty acid supplement use with cardiovascular disease risks: meta-analysis of 10 trials involving 77 917 individuals. *JAMA Cardiol* 2018;**3**:225–234.
46. Fredman G, Hellmann J, Proto JD, Kuriakose G, Colas RA, Dorweiler B, Connolly ES, Solomon R, Jones DM, Heyer EJ, Spite M, Tabas I. An imbalance between specialized pro-resolving lipid mediators and pro-inflammatory leukotrienes promotes instability of atherosclerotic plaques. *Nat Commun* 2016;**7**:12859.
47. Elajami TK, Colas RA, Dalli J, Chiang N, Serhan CN, Welty FK. Specialized proresolving lipid mediators in patients with coronary artery disease and their potential for clot remodeling. *FASEB J* 2016;**30**:2792–2801.
48. Colas RA, Dalli J, Chiang N, Vlasakov I, Sanger JM, Riley IR, Serhan CN. Identification and actions of the Maresin 1 metabolome in infectious inflammation. *J Immunol* 2016;**197**:4444–4452.
49. Souza PR, Marques RM, Gomez EA, Colas RA, De Matteis R, Zak A, Patel M, Collier DJ, Dalli J. Enriched marine oil supplements increase peripheral blood specialized pro-resolving mediators concentrations and reprogram host immune responses: a randomized double-blind placebo-controlled study. *Circ Res* 2020;**126**:75–90.
50. Sun YP, Oh SF, Uddin J, Yang R, Gotlinger K, Campbell E, Colgan SP, Petasis NA, Serhan CN. Resolvin D1 and its aspirin-triggered 17R epimer. Stereochemical assignments, anti-inflammatory properties, and enzymatic inactivation. *J Biol Chem* 2007;**282**:9323–9334.
51. Hong S, Porter TF, Lu Y, Oh SF, Pillai PS, Serhan CN. Resolvin E1 metabolome in local inactivation during inflammation-resolution. *J Immunol* 2008;**180**:3512–3519.
52. Cicha I, Chauvierre C, Texier I, Cabella C, Metselaar JM, Szebeni J, Dezsi L, Alexiou C, Rouzet F, Storm G, Stroes E, Bruce D, MacRitchie N, Maffia P, Letourneur D. From design to the clinic: practical guidelines for translating cardiovascular nanomedicine. *Cardiovasc Res* 2018;**114**:1714–1727.

Downloaded from academic.oup.com/cardiovascres/article/122/3/397/8430176 by Ewha Womans University Library - (INACTIVE) user on 28 August 2026